Interaction of Mant-Adenosine Nucleotides and Magnesium with Kinesin†

Jing-Qui Cheng, Wei Jiang, and David D. Hackney*

Department of Biological Sciences, Carnegie Mellon University, Pittsburgh, Pennsylvania 15213

Received October 21, 1997; Revised Manuscript Received February 12, 1998

ABSTRACT: Displacement of the fluorescent substrate analogue methylanthraniloyl ADP (mant-ADP) from kinesin by excess ATP results in a biphasic fluorescent transient. The pH and microtubule dependence of the rates and amplitudes indicates that the two phases are produced by release of bound mant-ADP, with an excess of the 3′-isomer, followed by the subsequent relaxation of the free 2′- and 3′-isomers to their equilibrium distribution. The first phase for release of mant-ADP is accelerated by microtubules and occurs at the same rate as ADP release measured using [^{32}P]ADP. The second phase is subject to base catalysis and occurs at the same rate as the isomerization of isolated 2′- or 3′-mant-ATP over a 100-fold range of rates. The bound mant-ADP isomers undergo isomerization rapidly when bound to kinesin at pH 8.2, whereas mant-ADP isomers interconvert only slowly when bound to myosin. No fluorescence resonance energy transfer occurs between the single tryptophan in the kinesin neck domain and bound mant-ADP, but efficient energy transfer does occur from protein tyrosine groups. The rate of mant-ADP release in the absence of microtubules is minimal (0.005 s^{-1}) at pH 7−8, 2 mM Mg^{2+}, and 25 mM KCl but is accelerated at lower pH (0.04 s^{-1} at pH 5.5) and either lower or higher [KCl] (0.01 and 0.06 s^{-1} at 0 and 800 mM KCl, respectively). The microtubule-stimulated rate of ADP release is accelerated at low pH and inhibited by high concentrations of monovalent salts. Reduction of the free Mg^{2+} by addition of excess EDTA increases the release of mant-ADP from E·MgADP to 0.03 s^{-1}. This acceleration at low Mg^{2+} likely represents sequential release of Mg^{2+} at 0.03 s^{-1} followed by rapid release of ADP, as the rate of ADP release from Mg-free E·ADP is fast (>0.5 s^{-1}). At high Mg^{2+}, rebinding of Mg^{2+} to E·ADP forces release of ADP from the E·MgADP complex at 0.005 s^{-1}.

Mant[1] nucleotides have been useful in the investigation of a number of enzymes (see ref *1*) including kinesin (*2*−*8*), myosin (*9*−*11*), Ras GTPase (*12*−*14*), and the Rep helicase (*15*). Mant nucleotides are present in solution as a mixture of the 2′- and 3′-isomers that undergo base-catalyzed interconversion with a half-life of minutes at neutral pH (*9*, *12*, *13*). The 3′-isomer is slightly favored [∼2:1 for 3′:2′ ratio of mant-ATP determined by proton NMR (*9*)] and has a higher fluorescence intensity. The isomers can be separated by reversed-phase HPLC at low pH where the isomerization reaction is slow (*12*, *13*). Standard kinetic analysis with the mixed isomers has the limitation that the rates for the two isomers can be different, although it is also possible to use single isomer analogues such as 2′-deoxy-3′-mant-ADP, if they are reasonable analogues of ATP. With Ras, it has been possible to determine that the 3′-isomer is bound more strongly (9:1 for the bound 3′:2′ ratio).

Our preliminary investigation of the fluorescence changes accompanying binding and release of mant-nucleotides to kinesin indicated that the fluorescence transients were biphasic and changed in a complex manner with variation in pH, ionic strength and MT concentration. Analysis of the kinetics of the individual 2′- and 3′-mant nucleotide isomers indicates, as reported here, that the complexity was produced by preferential binding of the 3′-isomer by kinesin. Determination of the rate of isomerization under different conditions of pH and concentration of KCl and Mg^{2+} has allowed the extraction of the basal rate of mant-ADP release under these conditions, independent of the complicating isomerization transient. This analysis indicates that Mg^{2+} can be released from the E·MgADP complex independent of release of ADP, unlike the case of myosin where Mg^{2+} is released as the complex with ADP or in rapid succession (*16*, *17*).

MATERIALS AND METHODS

Head domains of *Drosophila* kinesin from amino acid position 1 to a series of termination sites (designated by DKHnnn, where nnn is the terminating amino acid position) were prepared as described in ref *18*. Human K349 (*19*) was prepared by the same method using a plasmid provided by R. D. Vale. Nucleotide-free protein was prepared by washing with EDTA buffer while bound to phosphocellulose essentially as described by Ma and Taylor (*20*). MTs were prepared by polymerization of tubulin as described (*21*), and the concentration of MTs is reported as the corresponding concentration of tubulin heterodimers. Myosin chymotryptic subfragment-1 was prepared as described (*22*). A25 buffer

† This work was supported by Grant NS28562 from the National Institute of Neurological Disorders and Stroke, National Institutes of Health.

* Author to whom correspondence should be addressed.

[1] Abbreviations: mant-ATP and mant-ADP, 2′(3′)-*O*-(*N*-methylanthraniloyl)adenosine 5′-triphosphate and -diphosphate respectively; 2′-mant and 3′-mant, the 2′-and 3′-isomers of mant-nucleotides; MT, microtubule; DKHnnn, designates a construct consisting of the first nnn amino acids of *Drosophila* kinesin; K349, the construct consisting of the first 349 amino acids of human kinesin; FRET, fluorescence resonance energy transfer.

S0006-2960(97)02742-6 CCC: $15.00
Published on Web 03/26/1998

Table 1: Release of mADP from E·Mg·mADP

Mg^{2+} in medium	DKH365[a] (/s)	S1[b] (/s)
(+)	0.0025	0.56
(−)	0.026	0.65

[a] Data for DKH365 from Figure 6 evaluated at approximately equivalent ionic strengths (50 mM KCl without magnesium versus 12.5 mM MgAcetate and 25 mM KCl). [b] For S1, the mADP complex in A25 buffer with 25 mM KCl was mixed with an equal volume of either the same buffer with 0.4 mM MgATP or with 25 mM Aces/KOH (pH6.9) containing 25 mM KCl, 4 mM EDTA, and 0.8 mM ATP. Done in triplicate with SE < 5%. Final free Mg^{2+} at approximately 1.9 and 0.003 mM, respectively.

contained 25 mM potassium ACES, pH 6.9, 2 mM magnesium acetate, 2 mM potassium EGTA, 0.1 mM potassium EDTA, and 1 mM 2-mercaptoethanol. Where indicated, PEP and MgATP were added from concentrated stock solutions. The PEP stock was prepared from monopotassium PEP and was adjusted to pH 7 by addtition of KOH. The MgATP stock was prepared by addition of 1 equiv of magnesium acetate/equiv of disodium ATP and then adusted to pH 7 by addition of KOH. All reactions were performed at 25 °C.

Mant-ATP and mant-ADP were prepared and purified by chromatography on Sephadex LH-20 essentially as described by Hiratsuka (*23*). The 2′- and 3′-isomers of mant-ATP were separated by HPLC on a Waters NovaPac C18 reversed-phase column using 20 mM potassium phosphate, pH 5.0, and 9.3% acetonitrile as described for mant-GTP (*13*, *14*).

Mant-ADP Release. Mant-ADP release was monitored by the fluorescence change following dilution of a stock of E·mant-ADP complex into buffer at 25 °C containing an excess of unlabeled nucleotide (1 mM MgATP except as indicated) as a chase. The stock of kinesin with bound mant-ADP was prepared by exchange of bound ADP for mant-ATP with subsequent hydrolysis to mant-ADP. Typically, a kinesin head domain was incubated with a 5-fold excess of mant-ATP for 10 min at 25° C in A25 with 50 mM KCl and then dialyzed at 4 °C versus the same buffer with 1−10 μM mant-ATP. It was necessary to maintain a significant level of free mant-nucleotide during dialysis in order to prevent the inactivation that occurs in the absence of nucleotide (*24*), but the concentration of kinesin head domain was typically ≥10-fold greater than the concentration of mant-ATP in the dialysis and, thus, most of the mant-ADP present at equilibrium will be bound to the head domain. The data were fit to various models as indicated using the Marquardt−Levenberg algorithm as implemented by the SigmaPlot program (Jandel).

Fluorescence spectra and slow kinetic experiments were performed in most case, on a SLM 8000 spectrofluorimeter. Excitation and emission were at 356 and 445 nm, respectively, except as indicated. Fluorescence was obtained in the ratio mode with the fluorescence of the sample normalized to the fluorescence of a rhodamine standard that was excited by the same light source. For slow reactions, the excitation slit width was ≤4 nm to minimize photobleaching. Reactions were stirred by a magnetic stirring bar during observation. The rate of mant-ADP release from S1 (Table 1) was obtained on a custom-made stopped-flow apparatus. Excitation was by a 100 W Hg-arch lamp with Schott UG-11 and WG320 filters for excitation (broad band in 356 nm region) and K418 and BG-39 filters for detection of emission

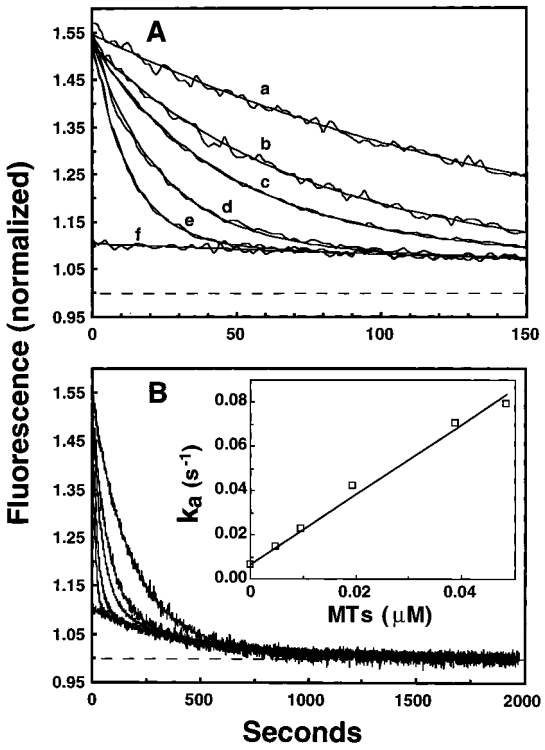

FIGURE 1: Release of mant-ADP from DKH357 at pH 6.9. The reaction was initiated by addition of E·mant-ADP to A25 buffer containing 25 mM KCl, 2 mM PEP, 1 mM MgATP, and 10 μM paclitaxol. The final concentration of DKH357 was 100 nM, and MTs were present at 0, 4.9, 9.7, 19.4, 48.4, and 775 nM for traces a−f, respectively. Excitation and emission were at 356 and 445 nm. The fluorescence for each trace was corrected for the blank level in the absence of E·mant-ADP and then normalized to the value at 2000 s. Panels A and B are the same data plotted on different time scales for clarity. Theoretical fits were calculated as described in the Results with k_b fixed at 0.0025 s^{-1}. The inset to panel B gives the value of k_a determined from the fit.

by a Thorn EMO Gencom photomultiplier tube (9924QB) with a high voltage power supply (3000R) and inverting preamplifier (A1). Two light guides were used to carry the excitation and emission light to and from the cell. A gas piston was used for driving two syringes into a T-mixer attached to a 2 × 2 mm quartz flow cell. A stop syringe was used to stop the flow and trigger data acquision by a Macinitosh computer using a PCI-1200 data acquisition board under the control of LabView software (National Instruments).

RESULTS

Characterization of Mant-ADP Release Using Excitation at 356 nm. Dilution of a complex of DKH357 and mant-ADP (E·mant-ADP) into media containing excess ATP results in a decrease in fluorescence (Figure 1) as the bound mant-ADP is released and replaced with ADP formed by hydrolysis of ATP. The amplitude of the total fluorescent decrease is ∼53% of the final value, and this decrease is similar to that observed with release of mant-ADP from other kinesin constructs (*5*, *6*). Inclusion of low levels of MTs in the chase accelerates the rate of the fluorescence decrease, but the process becomes markedly biphasic. At high levels of MTs (trace f), the MT-stimulated phase is completed within the mixing time, but a MT-insensitive component remains with rate constant of 0.0025 s^{-1} and an amplitude of 10% of the final value.

The data were fit to a sequential model (*25*)

$$A \xrightarrow{k_a} B \xrightarrow{k_b} C$$

that corresponds to the scheme developed below with the first step accelerated by MTs and the second step independent of MTs. The curves in Figure 1 were all fit to this model with the only constraint being that k_b was fixed at the value of 0.0025 s^{-1} that is observed at saturating MT levels in trace f. The fits indicated that the amplitude of the second step was between 8.9 and 10.3% in all cases and thus is independent of the MT concentration. The observed amplitudes are expected to be slightly less than the true amplitudes due to the presence of a low level of free mant-ADP in the dialyzed stock of E·mant-ADP. The k_a value was linearly dependent on the MT concentration as indicated in the insert to Figure 1B. The k_o and k_{bi}^{ADP} values for $k_a = k_o + k_{bi}^{ADP}$ [MTs] were 0.0063 s^{-1} and 1.59 μM^{-1} s^{-1}, respectively. The k_o value for the rate of release of mant-ADP in the absence of MTs is approximately equal to the rate for ADP release of 0.005 s^{-1} determined using [^{32}P]-ADP (*18*). Essentially identical results have been obtained with DKH346, DKH365, and dimeric DKH392 and DKH405, except that the k_{bi}^{ADP} values vary greatly (0.95, 17.7, 11.5, and 3.9 μM^{-1} s^{-1}, respectively) as is also observed for MT-stimulated ADP release in 120 mM potassium-acetate (*18*).

The rates of the two phases, but not their amplitudes, are strongly dependent on pH. At both high and low pH, k_o and k_b differ significantly in rate, but their relative magnitude is reversed with $k_o \gg k_b$ at pH 6.4 and $k_o \ll k_b$ at pH 8.5. The dependence of k_o and k_b on pH is indicated in Figure 2A for DKH365. The k_o values increase sharply at low pH, but are largely independent of pH over the neutral to basic range. The k_b values increase steeply with increasing pH over the whole range. It is only in the neutral pH range that the k_o and k_b values are of comparable magnitude. The k_{bi}^{ADP} values increase sharply at lower pH as indicated in Figure 2C, although the midpoints for the transitions differ. The rate for DKH405 decreases over 70-fold between pH 6.4 and 8.5 (11−0.15 μM^{-1} s^{-1}, respectively).

Equilibration of 2′- and 3′-Mant-ATP Isomers. Mant-nucleotides are known to be composed of a mixture of the 2′- and 3′-isomers that undergo base-catalyzed interconversion (*9*, *12*, *13*). If kinesin bound one isomer preferentially, then the ratio of bound mant-ADP isomers would differ from the ratio of the free isomers in solution, and the MT-insensitive phase could result from the reequilibration of the free isomers following release from kinesin. To investigate this possibility, the 2′- and 3′-isomers were separated by HPLC as described for mant-GTP (*13*, *14*) at low pH where the equilibration is slow. The first peak to elute had higher relative fluorescence and as was assigned to the 3′-isomer (*1*). The 3′:2′ isomeric ratio of 1.6:1 based on the A_{254} of the two peaks is in reasonable agreement with the 2:1 ratio for mant-ADP determined by NMR (*9*). Addition of each isomer to A25 buffer with 25 mM KCl at pH 6.9 produced two reciprocal fluorescence transients with relative fluorescence of 0.54:1.32:1.00 for the 2′-isomer, 3′-isomer, and the equilibrium mixture. The 3′:2′ ratio at equilibrium is thus 1.44:1 as determined from the fluorescent amplitudes, in approximate agreement with the ratio determined by HPLC. The rate of equilibration of both isomers (k_{iso}) is equal at

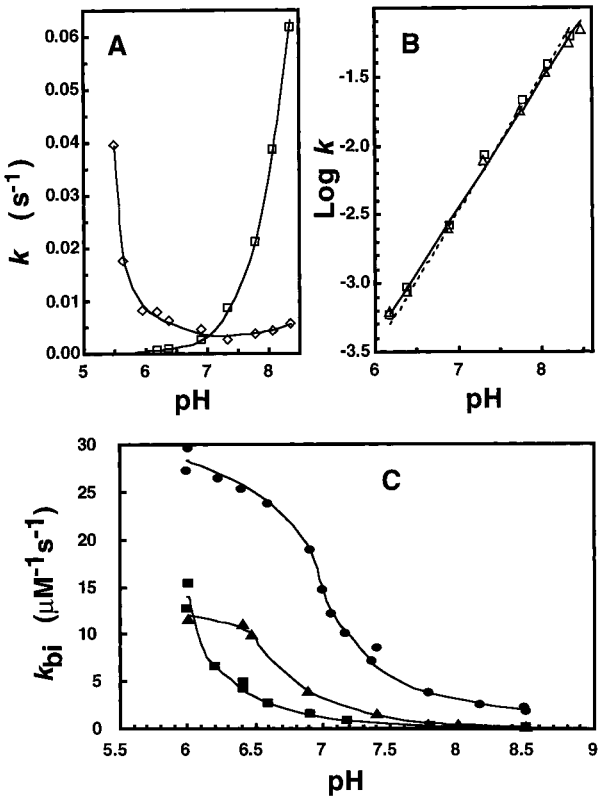

FIGURE 2: Dependence of rate constants on pH. The k_o, k_b, k_{bi}^{ADP}, and values were determined essentially as described in Figure 1. At pH values below 6, k_b was too slow to measure and k_o was determined by fitting to a single exponential with a slow linear drift component. The value of k_{iso} was determined from equilibration of the separated isotopes. All reactions contained 25 mM KCl. The pH 6.9 buffer was A25. Other buffers were identical to A25 except that the 25 mM ACES was replaced with 25 mM MES (pH <6.9), 25 mM HEPES (pH 7−8.3), 35 mM Tris (pH >8.3 for panels A and B) or 25 mM HEPPS (pH >8 for panel C). (A) Dependence of k_o (◇) and k_b (□) on pH for DKH365. (B) Dependence of log k_b (open square) for DKH365 and k_{iso} (open triangle) on pH. Solid line is a fit to all of the data with a slope of 0.93. The dashed line is a theoretical line with slope of 1 for comparison. (C) Dependence of k_{bi}^{ADP} on pH for DKH357 (■); DKH365 (●); and DKH405 (▲).

0.0023−0.0026 s^{-1} and this is also equal to the rate of the MT-insensitive phase, k_b, of 0.0025 s^{-1} observed in Figure 1 under similar conditions.

Both k_{iso} and k_b are subject to base catalysis with an approximately linear dependence on the concentration of [OH^-] as indicated in Figure 2B. The equality of the rate constants for k_b and k_{iso} over a greater than 100-fold change in absolute rate strongly suggests that the MT-insensitive phase, that is characterized by k_b, is due to equilibration of the free mant-ADP isomers, after their release from kinesin at a perturbed ratio. The observed total fluorescent transient thus likely represents the MT-stimulated release of mant-ADP from kinesin, k_a, with an amplitude decrease of ∼45%, followed by equilibration of the free isomers, $k_b = k_{iso}$, with a further amplitude decrease of ∼10% (both expressed relative to the fluorescence of the free isomers at equilibrium). Addition of nucleotide-free DKH357 to mant-ADP produces a fluorescence enhancement of ∼65% that is larger than the ∼55% enhancement observed in Figure 1. This difference is at least in part due to the presence of free mant-ADP in the dialzyed stock of E·mant-ADP used in Figure 1.

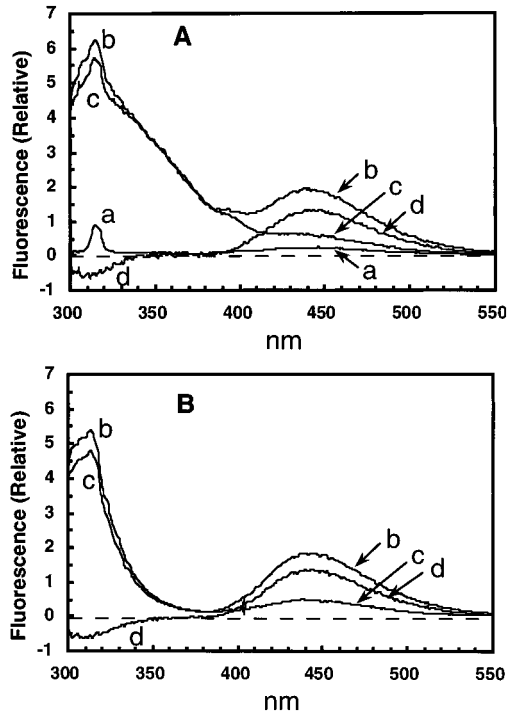

FIGURE 3: Emission spectra of E·mant-ADP. Emission spectra were obtained at an excitation wavelength of 285 nm in A25 buffer with 25 mM KCl. (A) Spectra with DKH357. (a) 1 μM mant-ATP, (b) 1 μM mant-ATP with 0.5 μM DKH357·mant-ADP; (c) Sample in trace b after 25 min chase with 20 μM ATP; (d) difference spectrum of b minus c. (B) Spectra with DKH346·mant-ADP. As in panel A for DKH357, but with DKH357·mant-ADP replaced with DKH346·mant-ADP and without repeat of trace a.

Fluorescence Energy Transfer. Excitation at 280 nm of complexes of mant nucleotides with myosin (*10*) and Rep helicase (*15*) results in fluorescence of the mant nucleotide at 445 nm by FRET. Similar energy transfer is observed with kinesin as a new excitation peak is observed at 280 nm only in the presence of both mant-ATP and kinesin (not shown). In the case of myosin, transfer occurs predominately from tryptophan, but this is not the case for kinesin as indicated in Figure 3. In this experiment, a low level of free mant-ATP was initially present in order to maintain saturation of kinesin with mant-ADP. This free mant-ATP did not have significant fluorescence when excited at 285 nm (trace a). Addition of the DKH357·mant-ADP complex in Figure 3A resulted in protein fluorescence at 300−400 nm and a second peak at 445 nm due to energy transfer to mant-ADP (trace b). The fluorescence at 445 nm was due to bound mant-ADP as it was selectively reduced by a chase with ATP (trace c). The difference spectrum (trace d) indicates that energy transfer resulted in quenching at 300−330 nm, but no quenching was observed in the 330−380 region of tryptophan fluorescence. That the energy transfer is independent of tryptophan is supported by the observation in Figure 3B that DKH346·mant-ADP has a FRET peak of the same amplitude even though DKH346 completely lacks tryptophan and has a greatly reduced level of protein fluorescence in the 330−390 nm region.

When excited at 285 nm, the transient for mant-ADP release from kinesin head domains obey simple first-order kinetics in the absence of MTs with a rate constant of ~0.005 s^{-1} and a large amplitude change of 600%. There is no MT-insensitive phase following rapid mant-ADP release stimulated by MTs (not shown) and the loss of the MT-insensitive phase is consistent with the reduced contribution of the free isomers to the energy transfer signal. The equal values of ~0.005 s^{-1} in the absence of MTs obtained at 285 nm and the k_a value obtained from analysis at 356 nm supports the identification of k_a as the rate of release of mant-ADP. Similar results have been obtained with other kinesin constructs (not shown). *Drosophila* kinesin head domains do not show an increase in fluorescence on binding of 2′-deoxy, 3′-mant-ATP when excitation is at 356 nm, in agreement with the results of Ma and Taylor with human kinesin (*2*). Bound 2′-deoxy, 3′-mant-ADP does still, however, yield a FRET signal when excitation is at 280 nm. The kinetics of release of 2′-deoxy, 3′-mant-ADP obtained with FRET are similar to those for release of the 2′-hydroxy nucleotides (not shown).

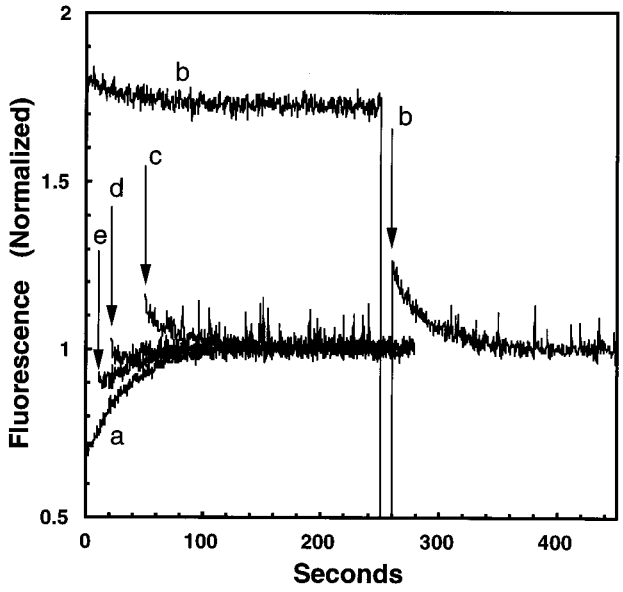

FIGURE 4: Binding of 2′-mant-ADP to nucleotide-free K349. All traces were initiated by addition of 2′-mant-ADP (0.15 μM) at zero time to 25 mM Hepes/KOH (pH 8.2) with 25 mM KCl, 2 mM magnesium acetate, 2 mM EGTA, and 0.1 mM EDTA. Trace a is 2′-mant-ADP alone. Traces b−e also contained nucleotide-free human K349 (0.7 μM). At the arrows, the bound mant-ADP was rapidly chased off by addition of MTs and MgATP to 2.5 and 200 μM, respectively. All traces are normalized to the value for the free isomers observed at 500 s. The parts of traces b−d before the chase are essentially identical to that of trace b and were omitted for clarity. Excitation was at 356 nm.

Comparison to Human K349. Detailed analysis of the nucleotide binding of DKH357 is complicated by the instability of nucleotide-free *Drosophila* kinesin, which undergoes a transition to a conformation that is not capable of rapidly rebinding ATP (*24*). Nucleotide-free kinesin from bovine (*26*) and human (*20*) sources, however, retain the ability to rapidly rebind ATP, and some comparative studies with human K349 were also performed. Initial experiments with human K349 indicated that its kinetics were highly similar to those of *Drosophila* DKH357, which terminates at the homologous position. In A25 buffer with 25 mM KCl, the k_{bi}^{ATPase} and k_{bi}^{ADP} values for K349 were 6.4 and 1.3 μM^{-1} s^{-1}, whereas the corresponding values for DKH357 were 7.3 (*18*) and 1.5 μM^{-1} s^{-1}.

The interaction of nucleotide-free human K349 with the 2′-mant-ADP isomer at pH 8.2 is indicated in Figure 4.

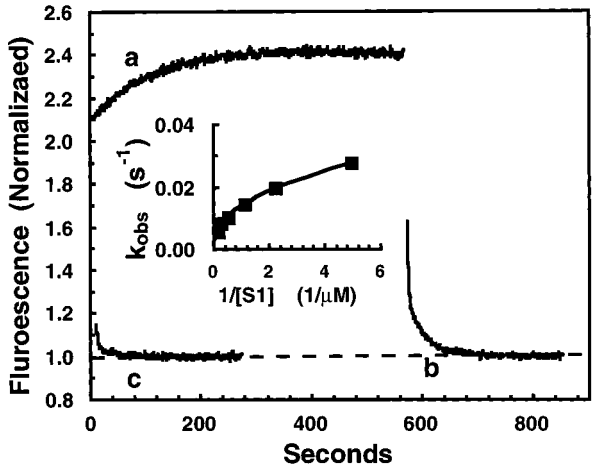

FIGURE 5: Equilibration of isomers bound to S1. For trace a, S1 was added to mant-ADP (1.8 and 0.3 μM, respectively) in the pH 8.2 buffer used in Figure 4. Trace b is a continuation of trace a following addition of 0.5 mM ATP. Trace c is similar, but an ATP chase was added after 10 s. Excitation was at 356 nm. The inset is the observed rates for the fluorescence increase corresponding to trace a, performed with different S1 concentrations.

Addition of 2-′mant-ADP to K349 produces a large enhancement that only decreases slightly during 250 s (trace b). Subsequent addition of MTs and ATP produces a biphasic fluorescence transient that is analogous to trace f of Figure 1 with rapid release of the bound mant-ADP followed by equilibration of the free isomers. The amplitude of the equilibration phase following the chase is larger than that for *Drosophila* heads (0.24 versus 0.10) and this indicates that the equilibrium of the bound species more strongly favors the 3′-isomer. Addition of MTs and ATP at shorter times (traces c, d, and e) indicates that the excess of bound 3-′mant-ADP builds in even more rapidly than the equilibration of free isomers (trace a). Under these conditions there is little free mant-ADP before the chase and thus the rapid equilibration of the isomers must occur while bound to K349. The MT activation of release of the separate isomers was determined in A25 buffer with 25 mM KCl by initiating a chase with MTs and ATP within 2−3 s after adding the 2′- or 3′-isomer to nucleotide-free K349. At 74 nM MTs, the release rates were 0.111 ± 0.001 and 0.092 ± 0.005 s^{-1} for the 2′- and 3′-complexes, respectively.

Comparison to Myosin S1. When an equilibrium mixture of mant-ADP isomers is added to nucleotide-free S1, there is an initial fluorescence enhancement on binding followed by a slower further increase (trace a, Figure 5). Addition of excess ATP as a chase (trace b) results in a biphasic transient. The fast phase is due to mant-ADP release which is known to be fast (*10*) and stopped-flow experiments in this buffer indicate that it has a rate of 0.56 s^{-1} (see below). The slow phase has the rate constant expected for equilibration of the released isomers and the amplitude of ≥0.25 indicates that the equilibrium of bound species strongly favors the 3′-isomer. An excess of 3′-isomer is not observed if the mant-ADP is chased off at short times (trace c), and incubations for varied times (not shown) indicate that the build up of excess bound 3′-isomer has the same kinetics as the increase in fluorescence observed in trace a. The increase in trace a indicates that the bound 3′-isomer has higher fluorescence than the bound 2′-isomer. The rate for the transient in trace a is 0.01 s^{-1} and this is slower than the isomerization rate of the free isomers (0.04 s^{-1}). Even this overestimates the true rate for isomerization of the bound species because part of the observed rate of isomerization is due to exchange between the bound and free species. Increasing the concentration of S1 should decrease the pool of free mant-ADP and decrease the contribution of exchange to net equilibration. The extrapolated equilibration rate at infinite concentration of S1 is ≤0.004 s^{-1} (insert to Figure 5) and thus the true isomerization rate of the isomers is over 10-fold slower when bound to S1 than when free.

Influence of Salt and Mg^{2+} on Basal ADP Release. The rate of release of mant-ADP from the E·Mgmant-ADP complex in the absence of MTs is accelerated at both low and high concentrations of KCl and inhibited by Mg^{2+} at all KCl concentrations (Figure 6A). In these experiments, kinesin with bound mant-ADP was equilibrated against buffer with 2 mM magnesium acetate and thus is present as the Mgmant-ADP complex at the start of the reaction, whether or not excess EDTA is present during the chase. The principal influence of Mg^{2+} in the chase is to inhibit ADP release at all KCl concentrations. The rate of isomerization of the free mant-ATP isomers is not strongly influenced by either KCl or Mg^{2+} (not shown). Concentrations of magnesium above 5 mM do not produce additional inhibition (Figure 6B). For comparison, the rate of release of mant-ADP from S1·Mgmant-ADP complexes in the presence and absence of free Mg^{2+} were also determined and are indicated in Table 1. The rate with S1 in the presence of Mg^{2+} is considerably faster than for kinesin, but is not significantly accelerated in the absence of Mg^{2+}.

The net binding of ADP to kinesin is considerably weaker in the presence of excess EDTA (*26*), but net binding still occurs if the free mant-ADP level is sufficiently high. In the experiment of Figure 7, the K349·Mgmant-ADP complex was equilibrated with free mant-ADP for varying times in the presence of excess EDTA and then chased with a large excess of ADP. When the chase is added together with the addition of the head complex (trace b), the rate is 0.05 s^{-1}, and this rate is similar to that observed for DKH365 with excitation at 356 nm at equivalent ionic strength (Figure 6). In the absence of an immediate chase (trace a), the fluorescence remains high over a time period in which all of the mant-ADP should have been released at least once. After Mgmant-ADP is released, the Mg^{2+} will be trapped by the excess EDTA, and the continued high level of fluorescence energy transfer indicates that most of the enzyme has rebound Mg-free mant-ADP. Now addition of a chase of ADP (at ∼160 s) produces rapid release of most of the bound mant-ADP indicating that the release of mant-ADP from the Mg-free complex with K349 is fast and completed within the manual mixing time. Addition of the chase at intermediate times (traces c and d) indicates that the fraction of bound mant-ADP that is released in the rapid phase increases in parallel to the decrease in fluorescence at 0.05 s^{-1} observed in trace b. The slow decrease in fluorescence observed in trace a before the chase likely represents slow inactivation of the enzyme under these conditions. Similar fast release of mant-ADP after equilibration with EDTA has been observed with DKH365, but is complicated by much more rapid inactivation following dilution into excess EDTA (not shown). The small residual transient observed after the chase in trace a has the same

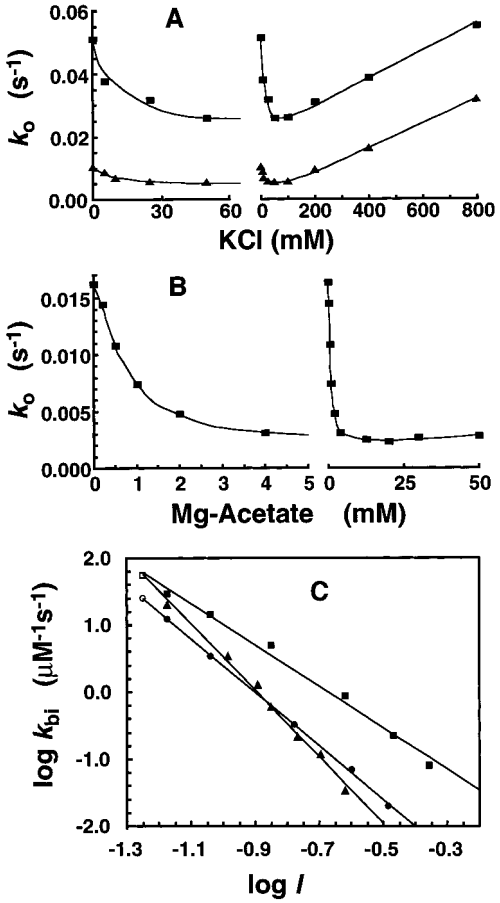

FIGURE 6: Influence of monovalent salts and magnesium on ADP release. The rate of release of mant-ADP was determined as described for k_o and k_{bi}^{ADP} in Figure 1 following dilution of kinesin·Mgmant-ADP into buffer containing different levels of monovalent salt and magnesium. In each case, the observed transient was fit to a sequential model constrained by the k_{iso} value for that condition. Panels A and B with DKH365. In panel A, the chase buffer was A25 (which contains 2 mM magnesium acetate) and 1 mM MgATP, (▲); or 25 mM Aces/KOH (pH 6.9), 0.5 mM EDTA and 1 mM Mg-free ATP (■). In panel B, the buffer was A25 with the normal 2 mM magnesium acetate replaced with varying levels of magnesium acetate as indicated. The buffer was also supplemented with 1 mM MgATP, 2 mM PEP, and 25 mM KCl. Note that the chase buffer in B contains 1 mM total magnesium (from the MgATP) even in the absence of added magnesium acetate. In panel C, the open symbols are for A25 buffer in the absence of added salt, but with 1 mM MgATP and 2 mM PEP for DKH365 (open square) and DKH392 (○). The closed symbols are with added KCl (▲) or potassium acetate (■) for DKH365 or with added KCl (●) for DKH392. The slopes are 4.97, 3.08, and 3.98, respectively.

rate constant as the larger transient in trace b and likely represents release from remaining K349·Mgmant-ADP.

Influence of Salt on MT-Stimulated ADP Release. Monovalent salts strongly inhibit bimolecular MT-stimulated ADP release as indicated in Figure 6C and Table 2. There are significant specific salt effects with chloride salts at 200 mM being over 10-fold more inhibitory than asparate or acetate salts for all cations tested (Table 2). The equilibrium binding of kinesin to MTs is also highly salt dependent (*5*), as is the MT-stimulated ATPase rate (*27*).

Comparison of Mant-ATPase and ATPase Kinetics. The kinetics of the mant-ATPase and the ATPase reaction have been reported to be similar for bovine (*4*), human (*20*), and rat (*6*) kinesin, and this is also true of *Drosophila* kinesin. The k_o rate for basal mant-ADP release and the k_{bi}^{ADP} rate

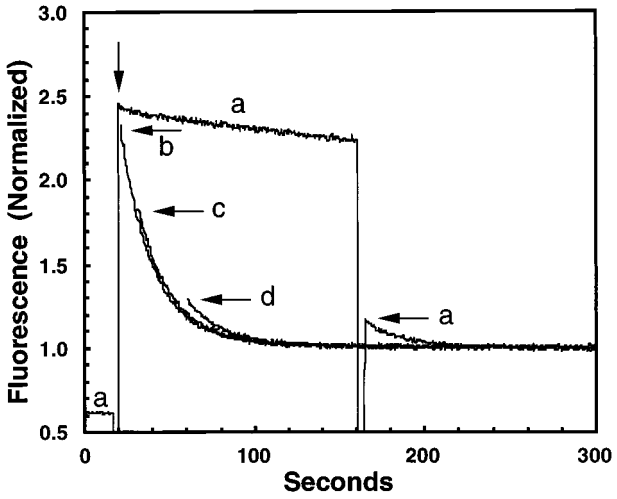

FIGURE 7: Release of mant-ADP from E·mant-ADP in excess EDTA. Trace a had initial conditions of 2.9 μM mant-ADP in 25 mM Aces/KOH (pH 6.9), 10 mM KCl and 1 mM EDTA. K349·Mgmant-ADP was added to 0.49 μM at the vertical arrow and chased off after 140 s by addition of Mg-free ADP to 100 μM at the horizontal arrow. Traces b−d are the chase phases for identical experiments except that the delay between addition of K349 and the chase was 0, 10, or 40 s, respectively. Excitation was at 285 nm. Values for each trace are normalized to value observed at 300 s. Control additions of ADP indicate that the small initial drop in fluorescence in trace b compared to trace a is due to the inner filter effect of the added ADP.

Table 2: Influence of 200 mM Monovalent Salts on k_{bi}^{ADP} [a]

	chloride (μM^{-1} s^{-1})	aspartate (μM^{-1} s^{-1})	acetate (μM^{-1} s^{-1})
potassium	0.042	0.55	0.86
ammonium	0.036	nd	0.52
sodium	0.024	nd	0.33
lysine	0.015	0.23	0.25

[a] Rate constant for MT-stimulated release of mant-ADP from DKH365 was determined as indicated in Figure 1 in A25 buffer with 1 mM MgATP, 2 mM PEP, and 200 mM of the indicated salt. nd is not determined. Standard errors of the fits were ≤10%.

for MT-stimulation of mant-ADP release were determined in A25 with 120 mM potassium-acetate for DKH357, DKH365, DKH392, and DKH405, and in all cases the values were within 15% of the corresponding values reported for unmodified ADP (*18*). It is not possible to use mant-ATP with the ATP regenerating system that has been used in most previous ATPase measurement of kinesin because mant-ADP is a poor substrate for pyruvate kinase. The ATPase and mant-ATPase rates were therefore determined by the initial rate of P_i release without a regenerating system for DKH405 as indicated in Table 3. The ATPase rates are essentially identical to the corresponding values determined with the ATP regenerating system (*18*). Although the rates for the mant-ATPase and the ATPase reactions are similar, the mant-ATPase has lower k_{cat} and k_{bi}^{ADP} rates and a higher $K_{0.5(MT)}$ value. The net result is that the lower k_{bi}^{ratio} value for mant-ATP predicts that kinesin has 40% less kinetic processivity with mant-ATP compared to ATP.

DISCUSSION

Mant nucleotides have proven to be valuable probes of numerous enzymes (see ref *1*), but their use is complicated by the presence of both 2′- an 3′-isomers that can intercon-

Table 3: Comparison of ATPase and Mant-ATPase of DKH405[a]

	ATPase	mant-ATPase
k_{cat} (s^{-1})	44.3 ± 0.1	35.3 ± 0.8
$K_{0.5}^{MT}$ (μM)	0.41 ± 0.03	0.59 ± 0.06
$k_{cat}/K_{0.5}^{MT} = k_{bi}^{ATPase}$ ($\mu M^{-1}s^{-1}$)	109	60
k_{bi}^{ADP} ($\mu M^{-1}s^{-1}$)	1.9 [b]	1.71 ± 0.04
k_{bi}^{ratio}	57	35

[a] Reactions were performed in A25 buffer with 120 mM potassium acetate, 2 mM PEP, and 1 mM MgATP or MgmantATP at 10 nM DKH405. Samples were quenched with cold perchloric acid to 0.83 M, centrifuged and the supernatant analyzed for P_i by the malichate green method (*31*). All rates were linear over the first 2 min. [b] From ref *18*.

vert. The detailed analysis presented here for the kinetics of the separate isomers indicates that they are very similar to each other and to unmodified ATP and ADP in their interactions with kinesin, but interesting quantitative differences exist between isomers and between their interactions with different enzymes.

In solution, the ratio of 3′:2′ isomers is ∼1.5:1 and the 3′-isomer is 32% more fluorescent than the equilibrium mixture. Binding to *Drosophila* kinesin shifts this ratio even more strongly in favor of the 3′-isomer as indicated by the 10% decrease in fluorescence that is observed during equilibration following rapid release of nucleotides (Figure 1, trace f). The results are consistent with a modest shift of the 3′:2′ ratio to 2.5:1 when bound to *Drosophila* kinesin. With human K349 (Figure 4) and myosin S1 (Figure 5), the corresponding decrease of 24−25% indicates a 3′:2′ ratio of ∼9:1 that is similar to the ratio reported for mant-GTP isomers bound to Ras (*12*, *13*). The data clearly indicate a large shift toward the 3′-isomer for human K349 and S1, but the exact ratio could be overestimated if the isolated 3′-mant-ATP, used to determine the limiting decrease of 32%, contained any 2′-isomer from incomplete HPLC separation or from isomerization at pH 5 before analysis. ADP release itself is likely to be a two step process (*2*), but these processes are too fast to be responsible for the biphasic kinetics observed here.

Kinesin, myosin, and Ras interact with both mant nucleotides and unmodified nucleotides in a similar manner that would be unlikely if the nucleotides bound in such a way that a large substituent on the ribose hydroxyls could not be accommodated without distorting the protein. In fact, the X-ray structures of nucleotide complexes of these enzymes indicate that the ribose hydroxyls are at least partially solvent exposed and could accommodate a substituent (*19*, *28*) as is observed in the structure of the complex of a mant-guanosine nucleotide with Ras (*29*). In particular, the ADP binding site of kinesin is largely open as discussed by Kull et al. (*19*) and illustrated in Figure 8. The 3′-hydroxyl points into solution with no close contact to protein residues (nearest protein atom is 6 Å away). The 2′-hydroxyl is in closer contact with kinesin and this may account for the preferential binding of the 3′-isomer, but the 2′-hydroxyl is still partially exposed and could accommodate a substituent directed away from the protein. Interconversion of the 2′- and 3′-mant-ADP isomers is more rapid when bound to kinesin than when free at pH 8.2 (Figure 4) in contrast to the slower rates of equilibration when bound to S1 (Figure 5) or Ras (*13*). Isomerization is base catalyzed in solution, and the bound

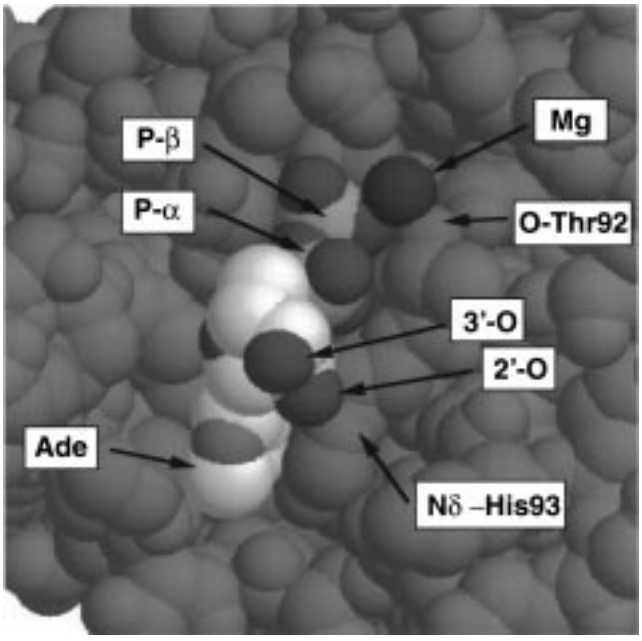

FIGURE 8: View of MgADP bound to kinesin. Image was generated from the coordinates of Kull et al. for human K349 with bound ADP (*19*) using RasMol (*32*). The protein is represented in spacefill mode with a uniform gray shading. The solvent water molecules that were defined in the X-ray structural determination are not included.

isomers could interconvert if they were exposed to solvent hydroxide or if protein side chains were properly oriented for general base catalysis. In this regard, it is interesting to note that kinesin has a His (H93 in human kinesin) near the ribose ring. The δ-nitrogen of its imidazole ring is only 3.23 Å away from the 2′-ribose hydroxyl in the X-ray structure (Figure 8) and is possibly hydrogen bonded. General base catalysis by H93 provides a reasonable potential mechanism for the acceleration of isomerization while bound to kinesin. The Ro value for FRET by the tryptophan/mant-nucleotide donor/acceptor pair has been estimated at ∼20 Å (*1*, *30*), and the failure to detect FRET (Figure 3) indicates that the distance between the single tryptophan in the neck of kinesin (Trp348 in *Drosophila* and Trp340 in human kinesin) and the active site is likely to be considerably longer than this.

The basal rate for mant-ADP release from *Drosophila* kinesin in the absence of MTs is very low at ∼0.005 s^{-1} in A25 buffer at pH 6.9, but increases markedly at low pH (Figure 2), high ionic strength, or low free magnesium concentration (Figure 6). With myosin, the ADP release rate is not accelerated at low free magnesium for either the MgADP−Pi products complex (*16*) or the MgADP complex [(*17*) Table 1], and this is interpreted to mean that MgADP is released as a complex or that both Mg^{2+} and ADP are rapidly released following some other rate-limiting step. The results with kinesin at moderate ionic strength are consistent with alternative pathways of either release of MgADP at 0.005 s^{-1} (as a complex or in rapid succession following a slower step) or release of Mg^{2+} at 0.03 s^{-1} that is followed by very rapid ADP release (Figure 7). High free Mg^{2+} suppresses ADP release by the sequential pathway because reversible rebinding of free Mg^{2+} can trap the Mg-free E·ADP complex before ADP is released. An alternative explanation is that there is a second Mg^{2+} binding site on kinesin whose occupancy influences the ADP release rate.

This possibility cannot be excluded, but there is no evidence for such a second Mg site, and none was observed in the X-ray structure (*19*).

The Mg^{2+} is also highly exposed to solvent in the kinesin·MgADP complex (Figure 8). It is ligated to the β-phosphoryl and to the hydroxyl of Thr92, but the other ligands are all solvent waters that largely fill the shallow depression above the Mg^{2+} in Figure 8. In contrast, the magnesium of the nucleotide complexes of S1 is largely buried inside a narrow channel that penetrates into the interior of the protein (*28*). These differences in magnesium binding may account for the differences in magnesium release between kinesin and S1 with the highly solvent exposed magnesium of kinesin being able to dissociate without linked dissociation of ADP, whereas the buried magnesium of the S1 complex cannot be readily released without a major conformational change that also facilitates release the ADP. Given the limited amount of contact of bound magnesium and ADP with kinesin, in fact, the problem is more to understand why the magnesium or ADP release rates are so slow as discussed by Kull et al. (*19*).

ACKNOWLEDGMENT

We thank the Drug Synthesis and Chemistry Branch of the National Cancer Institute for Taxol; A. Koretsky for use of the SML spectrofluorimeter; R. D. Vale for the clone of K349; M. Stock for isolation of proteins; J. Nagly for assistance in preliminary experiments, and F.J. Kull for coordinates of kinesin X-ray structure.

NOTE ADDED IN PROOF

Bauer et al. [Bauer, C. B., Kuhlman, P. A., Bagshaw, C. R., and Rayment, I. (1997) *J. Mol. Biol. 274*, 394−407] have recently described the X-ray crystal structure of mant-nucleotides bound to Dictyostelium S1 and find that the bound speices is predominantly the 3′ isomer.

REFERENCES

1. Jameson, D. M., and Eccleston, J. F. (1997) *Methods Enzymol. 278*, 363−390.
2. Ma, Y. Z., and Taylor, E. W. (1997) *J. Biol. Chem. 272*, 717−723.
3. Ma, Y. Z., and Taylor, E. W. (1997) *J. Biol. Chem. 272*, 724−730.
4. Sadhu, A., and Taylor, E. W. (1992) *J. Biol. Chem. 267*, 11352−11359.
5. Ma, Y. Z., and Taylor, E. W. (1995) *Biochemistry 34*, 13242−13251.
6. Lockhart, A., Cross, R. A., and McKilop, D. F. A. (1995) *FEBS Lett. 368*, 531−535.
7. Rosenfeld, S. S., Correia, J. J., Zing, J., Rener, B., and Cheung, H. C. (1996) *J. Biol. Chem. 271*, 30212−30221.
8. Gilbert, S. P., Webb, M. R., Brune, M., and Johnson, K. A. (1995) *Nature 373*, 671−676.
9. Cremo, C. R., Neuron, J. M., and Yount, R. G. (1990) *Biochemistry 29*, 3309−3319.
10. Woodward, S. K. A., Eccleston, J. F., and Geeves, M. A. (1991) *Biochemistry 30*, 422−430.
11. White, H. D., Belknap, B., and Jiang, W. (1993) *J. Biol. Chem. 268*, 10039−10045.
12. Eccleston, J. F., Moore, K. J. M., Bownbridge, G. G., Webb, M. R., and Lowe, P. N. (1991) *Biochem. Soc. Trans. 19*, 432−437.
13. Rensland, H., Lautwein, A., Wittinghofer, A., and Goody, R. S. (1991) *Biochemistry 30*, 11181−11185.
14. Moore, K. J. M., Webb, M. R., and Eccleston, J. F. (1993) *Biochemistry 32*, 7451−7459.
15. Moore, K. J. M., and Lohman, T. M. (1994) *Biochemistry 33*, 14550−14564.
16. Mandelkow, E.-M., and Mandelkow, E. (1973) *FEBS Lett. 33*, 161−166.
17. Bagshaw, C. R., and Trentham, D. R. (1974) *Biochem. J. 141*, 331−349.
18. Jiang, W., Stock, M., Li, X., and Hackney, D. D. (1997) *J. Biol. Chem. 272*, 7626−7632.
19. Kull, R. J., Sablin, E. P., Lau, R., Fletterick, R. J., and Vale, R. D. (1996) *Nature 380*, 550−555.
20. Ma, Y. Z., and Taylor, E. W. (1995) *Biochemistry 34*, 13233−13241.
21. Jiang, W., and Hackney, D. D. (1997) *J. Biol. Chem. 272*, 5616−5621.
22. Margossian, S. S., and Lowey, S. (1982) *Methods Enzymol. 85*, 55−71.
23. Hiratsuka, T. (1983) *Biochim. Biophys. Acta 742*, 496−508.
24. Huang, T.-G.; Hackney, D. D. (1994) *J. Biol. Chem. 269*, 16493−16501.
25. Fersht, A. (1984) *Enzyme Structure and Function*, W. H. Freeman, New York.
26. Hackney, D. D., Malik, A., and Wright, K. W. (1989) *J. Biol. Chem. 264*, 15943−15948.
27. Wagner, M. C., Pfister, K. K., Bloom, G. S., and Brady, S. T. (1989) *Cell Motil. Cytoskel. 12*, 195−215.
28. Fisher, A. J., Smith, C. A., Thoden, J. B., Smith, R., Sutoh, K., Holden, H. M., and Rayment, I. (1995) *Biochemistry 34*, 8960−8972.
29. Scheidig, A. J., Franken, S. M., Corrie, J. E. T., Reid, G. P., Wittinghofer, A., Pai, E. F., and Goody, R. S. (1995) *J. Mol. Biol. 253*, 132−150.
30. Leonard, D. A., Evans, T., Hart, M., Cerione, R. A., and Manor, D. (1997) *Biochemistry 33*, 12323−12328.
31. Penney, C. L., and Bolger, G. (1978) *Anal. Biochem. 89*, 297−303.
32. Sayle, R., and Milner-White, E. J. (1995) *Trends. Biochem. Sci. 20*, 374−374.

BI972742J